Front. Environ. Sci. Eng. 2023, 17(3): 29
https://doi.org/10.1007/s11783-023-1629-9

REVIEW ARTICLE

Bacteria inactivation by sulfate radical: progress and non-negligible disinfection by-products

Xin Zhou[1,2], Xiaoya Ren[1,2], Yu Chen[1,2], Haopeng Feng[1,2], Jiangfang Yu[1,2], Kang Peng[1,2], Yuying Zhang[1,2], Wenhao Chen[1,2], Jing Tang[1,2], Jiajia Wang (✉)[1,2], Lin Tang (✉)[1,2]

1 College of Environmental Science and Engineering, Hunan University, Changsha 410082, China
2 Key Laboratory of Environmental Biology and Pollution Control (Hunan University), Ministry of Education, Changsha 410082, China

HIGHLIGHTS

- Status of inactivation of pathogenic microorganisms by $SO_4^{\bullet-}$ is reviewed.
- Mechanism of $SO_4^{\bullet-}$ disinfection is outlined.
- Possible generation of DBPs during disinfection using $SO_4^{\bullet-}$ is discussed.
- Possible problems and challenges of using $SO_4^{\bullet-}$ for disinfection are presented.

GRAPHIC ABSTRACT

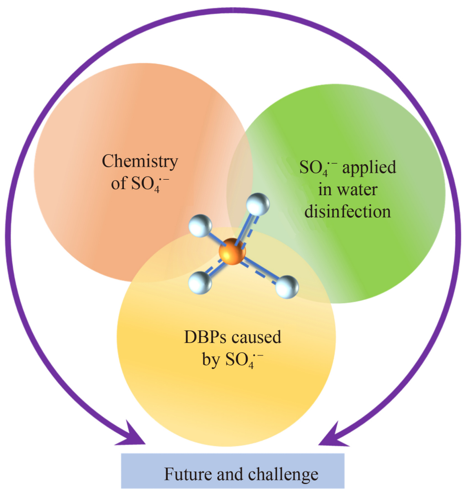

ARTICLE INFO

Article history:
Received 29 May 2022
Revised 19 August 2022
Accepted 22 August 2022
Available online 30 September 2022

Keywords:
Sulfate radicals
Disinfection by-products
Inactivation mechanisms
Bacterial inactivation
Water disinfection

ABSTRACT

Sulfate radicals have been increasingly used for the pathogen inactivation due to their strong redox ability and high selectivity for electron-rich species in the last decade. The application of sulfate radicals in water disinfection has become a very promising technology. However, there is currently a lack of reviews of sulfate radicals inactivated pathogenic microorganisms. At the same time, less attention has been paid to disinfection by-products produced by the use of sulfate radicals to inactivate microorganisms. This paper begins with a brief overview of sulfate radicals' properties. Then, the progress in water disinfection by sulfate radicals is summarized. The mechanism and inactivation kinetics of inactivating microorganisms are briefly described. After that, the disinfection by-products produced by reactions of sulfate radicals with chlorine, bromine, iodide ions and organic halogens in water are also discussed. In response to these possible challenges, this article concludes with some specific solutions and future research directions.

1 Introduction

Disinfecting is an important process to eliminate microorganism, pathogenic bacteria and other biological hazards (Anipsitakis et al., 2008; Xiao et al., 2019; Lei et al., 2021). Chlorination as the most used disinfection method commonly results in disinfection by-products (DBPs) and may be noneffective against resistant microorganisms (Wang et al., 2019; Wang et al., 2021; Liang et al., 2022; Zhao et al., 2022). In this case, current

✉ Corresponding authors
E-mails: wangjiajia07@hnu.edu.cn (J. Wang);
tanglin@hnu.edu.cn (L. Tang)

research focus has shifted to using reactive oxygen species (such as hydroxyl radicals, singlet oxygen, sulfate radicals, and superoxide radicals) which generated in advanced oxidation processes (AOPs) to degrade pollutants and inactivate pathogens due to their high redox potential (Zhang et al., 2010; Sun et al., 2016; Wang et al., 2017a; Wang et al., 2018; Yu et al., 2020). For example, Bai et al. (2022) explored the mechanism of superoxide radical ($O_2^{\bullet-}$) degradation of perfluorocarboxylic acid (PFCAs). The results revealed that the low polar solvent enhanced the nucleophilicity of $O_2^{\bullet-}$, but also reduced the desolvation process of PFCAs, leading to a decrease in kinetics. Cho et al. (2004) studied photocatalytic inactivation of bacteria with TiO_2, and found that the amount of hydroxyl radicals (•OH) has an excellent linear relationship with the degree of *E. coli* inactivation under constant temperature. Current research has demonstrated that generation of large amounts of •OH in Fenton's reaction requires a strictly acidic environment (pH 2–4) (Pignatello et al., 2006; Tang et al., 2022). Therefore, the practical application of Fenton's reaction in disinfection is extremely limited.

At present, sulfate radical ($SO_4^{\bullet-}$) was found to be a perfect substitution to •OH as its abilities in irreversibly destroying cell structure or function (Zhang et al., 2014; Sun et al., 2016; Xiao et al., 2020). $SO_4^{\bullet-}$ is generated by persulfate (PS) or peroxymonosulfate (PMS). Compared with hydrogen peroxide (H_2O_2) that forms •OH, solid PMS and PS are cheaper, more stable, and more convenient to store and transport (Wacławek et al., 2017). Meanwhile, $SO_4^{\bullet-}$ can selectively oxidize biomolecules and macromolecules with electron-rich groups, making it more suitable for inactivating microorganisms (Neta et al., 1988). There are more and more researches on sulfate radicals-based AOPs (SR-AOPs) in water disinfection in recent years, and promising results have been achieved (Rodríguez-Chueca et al., 2017b; Wen et al., 2017; Marjanovic et al., 2018; Zhou et al., 2018; Wu et al., 2019; Ferreira et al., 2020; Wang et al., 2020a). For example, Zhang et al. (2020) investigated the effect of sulfidated micron zero-valent iron/PS (S-mZVI/PS) system on the viability of inactivating *E. coli*. The results showed that 7–8 log *E. coli* was completely eliminated within 30 minutes after treated with 1 mmol/L PS and 40 mg/L S-mZVI.

Unfortunately, as a strong oxidant similar to •OH, $SO_4^{\bullet-}$ may react with halogen ions in water during disinfection to produce DBPs which can cause bladder cancer, colorectal cancer, miscarriage and birth defects (including heart defects found in 2016) (Richardson and Kimura, 2019). Fang and Shang (2012) firstly discovered that $SO_4^{\bullet-}$ can oxidize bromide (Br^-) to cancerogen bromate (BrO_3^-). Later, Lu et al. (2015) studied the conversion of bromide in the heat activated oxidation process of PS in the presence of humic acid (HA) and confirmed the formation of bromoform and bromoacetic acid. Under acidic conditions, chloride (Cl^-) has a similar conversion process in the UV/PS process, and $SO_4^{\bullet-}$ can also convert Cl^- into chlorate (ClO_3^-) which is harmful to humans (Lutze et al., 2015). Many studies use SR-AOPs for disinfection and sterilization without discussing the risks of generating DBPs which can not be ignored. Accordingly, based on the prospect and existing problems of sulfate radicals in the disinfection process, they are more suitable for the disinfection of aquaculture, swimming pool and ballast water.

Previous reviews on the topic of SR-AOPs in water disinfection, mainly focused on high-efficiency inactivation in the process, but few of them considered the impact of subsequent DBPs. Therefore, this review has mainly done the following work: 1) Briefly summarized the properties of sulfate radical; 2) Comprehensively reviewed the research on sulfate radical inactivation; 3) Discussed the possible formation of DBPs in the process; 4) Stated possible existence problems and future challenges.

2 Chemistry of sulfate radical

Table 1 lists the oxidation potentials of oxidants commonly used in water treatment. As displayed in the table, $SO_4^{\bullet-}$ is a strong oxidant with a standard redox potential of 2.5–3.1 V vs. NHE (normal hydrogen electrode), which is close to •OH (+2.80 V vs. NHE) (Lian et al., 2017). The half-life of the $SO_4^{\bullet-}$ is 30–40 μs, which is longer than •OH (10^{-3} μs) (Devasagayam et al., 2004). At the same time, $SO_4^{\bullet-}$ tends to react with organic matter in the process of electron transfer, while •OH participates in various reactions without selectivity (Ghanbari and Moradi, 2017). This means that $SO_4^{\bullet-}$ are more selective than •OH. Since sulfate radical is electrophilic, it prefers to react with electron-donating groups rather than electron-withdrawing groups (Hu and

Table 1 Oxidation potentials of oxidants commonly used in water

Oxidant	Oxidation potential (V)	Ref.
Fluorine	3.0	Guerra-Rodríguez et al., 2018
Hydroxyl radical	2.8	Wang and Wang, 2018
Sulfate radical	2.5–3.1	Ferreira et al., 2020
Ozone	2.1	Ao et al., 2021
Persulfate	2.0	Wacławek et al., 2017
Peracetic acid (PAA)	1.96	Ao et al., 2021
Peroxymonosulfate	1.8	Ao et al., 2021
H_2O_2	1.8	Ao et al., 2021
Potassium permanganate	1.7	Ao et al., 2021
Chlorine dioxide	1.5	Ao et al., 2021
Chlorine	1.4	Ao et al., 2021

Long, 2016). Generally, the reaction between $SO_4^{\bullet -}$ and organic molecules is very fast and the second-order rate constant is between 10^5 to 10^9 $M^{-1}\cdot s^{-1}$ (Neta et al., 1988; Oh et al., 2016). Sulfate radicals can react effectively with organic compounds with the similar reactivity in the pH range of 2–8 (Oh et al., 2016). In addition, the radicals can also react with water to generate •OH, and the reaction equation is as follows (Eqs. (1) and (2)) (Waldemer et al., 2007):

$$SO_4^{\bullet -} + H_2O \rightarrow SO_4^{2-} + \bullet OH + H^+,\ k < 1.0\times 10^3 M^{-1}\cdot s^{-1} \quad (1)$$

$$SO_4^{\bullet -} + OH^- \rightarrow SO_4^{2-} + \bullet OH,\ k = (6.5\pm 1.0)\times 10^7 M^{-1}\cdot s^{-1} \quad (2)$$

Equations (1) and (2) can occur at all pH conditions, but under alkaline conditions, the reaction of Eq. (2) is more pronounced. When pH > 8.5, $SO_4^{\bullet -}$ is rapidly decomposed into •OH, and when pH > 10.7, •OH becomes the dominant radical (Yang et al., 2010). In addition, the $SO_4^{\bullet -}$ can react with themselves (Eq. (3)) (Huie and Clifton, 1993). Due to the low concentration of $SO_4^{\bullet -}$, its self-scavenging effect can be ignored.

$$SO_4^{\bullet -} + SO_4^{\bullet -} \rightarrow S_2O_8^{2-},\quad k = 4\times 10^8 M^{-1}\cdot s^{-1} \quad (3)$$

3 Sulfate radical applied in water disinfection

Sulfate radical is mainly produced by PS and PMS activation. Moreover, the essential mechanism of PS and PMS activation is the O–O bond fracture in their structures (Wang and Wang, 2018). PS is easier to be activated than PMS, because the O–O bond of PS (0.149 nm) is longer than that of PMS (0.146 nm) (Hu et al., 2020). There are many activation methods, such as heat, UV, base, transient metals and carbon-based materials (Lei et al., 2015; Xiao et al., 2018). The effectiveness of SR-AOPs in degrading organic pollutants has been proven. In recent years, this technology has been applied to inactivate microorganisms and has exhibited good performance. It is considered as a valuable and promising technology in water disinfection.

3.1 Mechanisms for water disinfection

At present, the literature on $SO_4^{\bullet -}$ inactivating microorganisms is relatively limited, and the inactivation mechanism remains to be further studied. Wen et al. (2017) explored the inactivation mechanism of four fungal spores under UV and UV/PMS systems. Unlike the results of UV irradiation alone, when PMS was added to the system, the appearance of large amounts of DNA was detected outside the cells. They analyzed the cell morphology of the four fungi before and after the reaction (Fig. 1(a)). The results showed that in the presence of PMS, the spore structure was disrupted and the cell wall was significantly damaged. So far, the inactivate microorganisms with $SO_4^{\bullet -}$ are mainly explained by the destruction of cell membranes/cell walls, enzymes and genetic material (Xiao et al., 2019). The inactivation mechanism is illustrated in Fig. 1(b).

The process of microorganism inactivation is that $SO_4^{\bullet -}$ first modify bacterial cell membranes and cell walls to change their permeability, which accelerates the penetration of oxidants, and then destroy intracellular components. Subramanian et al. (2013) and Wang et al. (2020a) used agarose gel electrophoresis to prove that $SO_4^{\bullet -}$ damage genetic material. Studies have found that, certain components of microorganisms such as guanine are more likely to react with $SO_4^{\bullet -}$ instead of •OH (Roginskaya et al., 2016). In addition, the chain scission rate caused by $SO_4^{\bullet -}$ is much higher than that by •OH (Sonntag, 2006), which means that $SO_4^{\bullet -}$ cause more serious damage to DNA than •OH. Although Zhang et al. (2020) have found that the $SO_4^{\bullet -}$ disinfection system has a lipid peroxidation effect on cell membranes, due to the existence of symbiotic •OH, the lipid peroxidation effect of $SO_4^{\bullet -}$ alone needs to be further confirmed. In terms of protein oxidation, $SO_4^{\bullet -}$ can cause protein cross-linking (Fancy and Kodadek, 1999), attack the carboxyl groups in amino acids (Davies et al., 1984), and initiate free radical chain reactions. Gau et al. (2010) compared the oxidation of protein by $SO_4^{\bullet -}$ and •OH, and found that the modification and residue selectivity of the two were very similar. As a consequence, it can be roughly inferred that the process of inactivating microorganisms by $SO_4^{\bullet -}$ and •OH is similar. It seems that $SO_4^{\bullet -}$ can also penetrate into cells and cause intracellular reactive oxygen species (ROS) to continuously increase and cause cell death. However, the mechanism of $SO_4^{\bullet -}$ inactivating microorganisms needs further investigation.

3.2 Inactivation kinetics

The inactivation studies of *E. coli*, other bacteria and some fungi by SR-AOPs are summarized in Tables 2–4. It can be seen that different activation methods have different inactivation efficiency for microorganisms. Among them, the most studied subjects are UV activations of PS and PMS to produce $SO_4^{\bullet -}$ for water disinfection and inactivation of microorganisms, followed by transition metal activation. As we can see, iron is the most commonly used transition metals, followed by cobalt. The widely studied target microorganism is *E. coli*, regarded as an indicator of fecal pollution in aquatic environments (Xiao et al., 2020). Furthermore, it is easy to obtain and cultivate, and its structure and composition are representative (Qi et al., 2020). In addition, the inactivation of viruses, fungi and other bacteria such as *S. aureus*, *E. faecalis* and *B. mycoides* has also been studied.

Venieri et al. (2020) explored the inactivation effect of

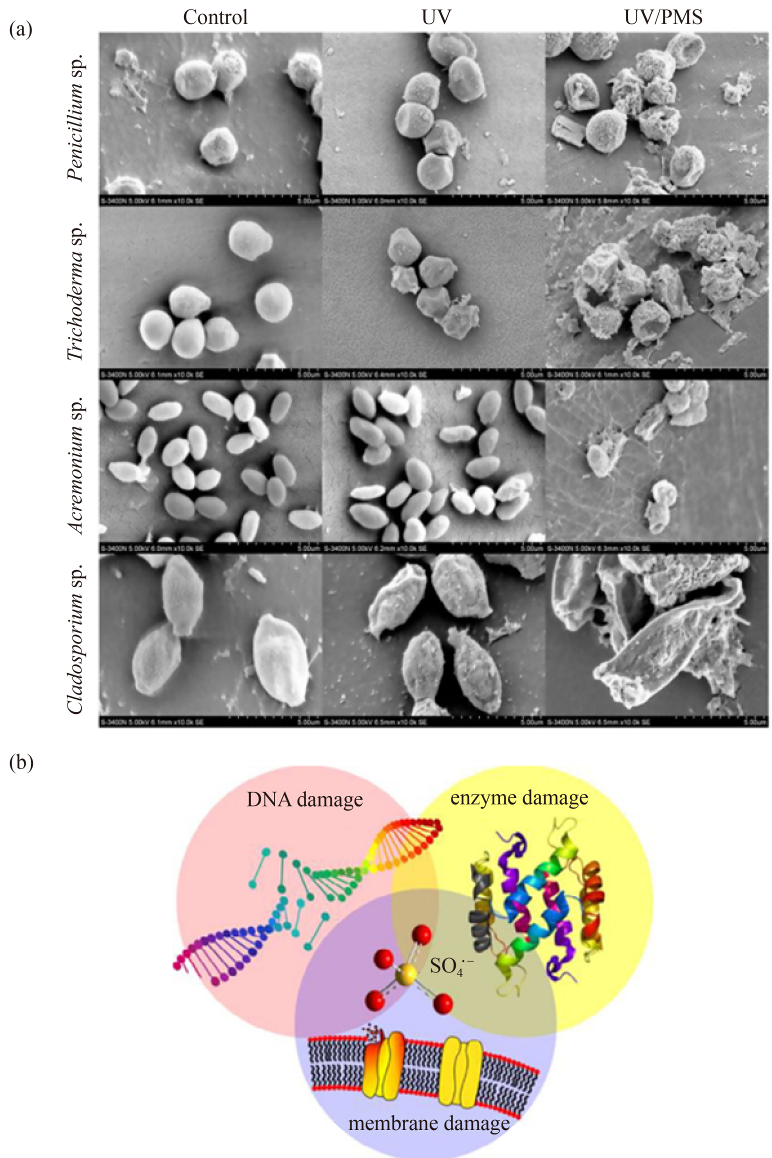

Fig. 1 (a) SEM images of fungal spores before and after treatment (control (left), UV (middle) and UV/PMS (right)). Experimental conditions: UV=40 mJ/cm^2, PMS=0.1 mmol/L, spore concentration=10^7 CFU/mL (Wen et al., 2017) (Copyright 2017 Elsevier, Reprinted with permission from Elsevier); (b) mechanism of inactivation of bacteria by sulfate radicals (Xiao et al., 2019) (Copyright 2019 Elsevier, Reprinted with permission from Elsevier).

UVA/PS on *E. coli* and found that 300 mg/L PS can inactivate 6 log of *E. coli* after UVA irradiation for 180 min. Rodríguez-Chueca et al. (2017b) investigated the inactivation efficiency of several bacteria by PMS under UV-A LED and fitted their inactivation kinetics. They found that Hom's model fits all results of bacterial inactivation. They also discovered that in the UV-A LED/PMS system, the Hom's kinetic rate constant of *E. coli* was the largest at 0.39 min^{-1}, followed by *S. aureus* (0.33 min^{-1}), and finally *B. mycoides* (0.06 min^{-1}). It may be explained by that the different structures of different bacteria lead to the difference of inactivation kinetic constants.

To control disinfection costs, Wang et al. (2019) explored the feasibility of sunlight /PS water disinfection. The results showed that VL/PS had a certain inactivation efficiency for bacteria (7 log reduction for *S. aureus*, *E. coli* and *P. aeruginosa*, after 200 min, 120 min and 140 min of VL irradiation with a PS dose of 2 mg/L, respectively). In their experiments, the log-linear-shoulder model was applied to fit the inactivation kinetics of VL/PS, thermal/PS, and VL/thermal/PS, and they found kinetic constants for these three systems to be 0.25 min^{-1}, 0.38 min^{-1}, and 1.29 min^{-1}, respectively. It can be concluded that the increase in temperature caused by sunlight exposure will further accelerate the process of bacterial inactivation. They also explored the effect of PS on the inactivation efficiency of *E. coli*, and found that the inactivation rate constant increased with the increase

Table 2 Summary of *E.coli* inactivation by SR-AOPs

Microorganisms	Initial conc. (CFU/mL)	System	Max. Log removal value	Dosage	Exposure time (min)	Ref.
E. coli	10^5	g-C_3N_4/VL/PMS	5	g-C_3N_4 0.1 g/L PMS 0.5 mmol/L	120	Zhang et al., 2021
E. coli	10^8	VL/PS/MHC	8	MHC 200 mg/L PS 2 mmol/L	40	Wang et al., 2020a
E. coli	10^7	UVA-LED/PMS	5.9	PMS 1 mg/L	60	Qi et al., 2020
E. coli	10^6	Fe^{3+}/PS	6	PS 200 mg/L Fe^{3+} 30 mg/L	15	Venieri et al., 2020
E. coli	10^6	50 °C/PS	6	PS 100 mg/L	60	Venieri et al., 2020
E. coli	10^6	UVA/PS	6	PS 300 mg/L	180	Venieri et al., 2020
E. coli	10^6	US/PS	6	PS 100 mg/L	120	Venieri et al., 2020
E. coli	10^6	PS/solar	6	PS 0.5 mmol/L	20	Ferreira et al., 2020
E. coli	10^6	US/Ag-BTO/PS	6.2	Ag-BTO_2 mg/mL PS 1 mmol/L	5 20(VBNC)	Xia et al., 2020
E. coli	10^7	CINMs/PMS	7	PMS 0.1 mmol/L	1	Shan et al., 2020
E. coli	10^7 to 10^8	S-mZVI/PS	completely eliminated	S-mZVI 40 mg/L PS 1 mmol/L	30	Zhang et al., 2020
E. coli	10^6	$CoFe_2O_4$/PMS/UVA	6	$CoFe_2O_4$ 0.05 g/L PMS 0.2 mmol/L	30	Rodríguez-Chueca et al., 2020
E. coli	10^7	VL/PS	7	PS 2 mmol/L	120	Wang et al., 2019
E. coli	10^7 to 10^8	3D-GFP	4.6	Na_2SO_4 50 mmol/L PS 2 mmol/L	10	Ma et al., 2019
E. coli	10^6	sunlight/Fe^{2+}/40 °C/PMS	6	1 mg/L Fe^{2+} 1.8×10^{-5} mol/L PMS	30	Rodríguez-Chueca et al., 2019a
E. coli	10^5	PMS/UVA	5	1 mmol/L PMS	30	Rodríguez-Chueca et al., 2019b
E. coli	10^5	PS/ Fe^{2+}/UVA	5	0.5 mmol/L PS 1 mg/L Fe^{2+}	2	Rodríguez-Chueca et al., 2019b
E. coli	10^7	PS/hv/ tris(2,2'-bipyridyl) ruthenium(II)	7	PS 2 mmol/L tris(2,2'-bipyridyl) ruthenium(II) 1 μmol/L	90	Subramanian et al., 2013
E. coli	9.2×10^5	PS/UV	3	PS 10 mg/L	5	Michael-Kordatou et al., 2015
E. coli	10^5	solar/PS/Fe^{2+}	3	PS 150 mg/L Fe^{2+} 5 mg/L	60	Garkusheva et al., 2017
E. coli	10^3 to 10^4	UVA/PMS/Fe^{2+}	4.2	0.1 mmol/L PMS 0.1 mmol/L Fe^{2+}	120	Rodríguez-Chueca et al., 2017a
E. coli	10^3 to 10^4	UVA/PMS/Co^{2+}	3.2	0.1 mmol/L PMS 0.1 mmol/L Co^{2+}	120	Rodríguez-Chueca et al., 2017a
E. coli	10^3 to 10^4	UVA/PMS/Fe^{2+}	6.5	0.1 mmol/L PMS 0.1 mmol/L Fe^{2+}	30	Rodríguez-Chueca et al., 2017b
E. coli	10^3 to 10^4	UVA/PMS/Co^{2+}	6.5	0.1 mmol/L PMS 0.1 mmol/L Co^{2+}	60	Rodríguez-Chueca et al., 2017b
E. coli	10^7	NP/PS	7	PS 1 mmol/L NP 1.25 g/L	20	Xia et al., 2017
E. coli	10^5	Ilmenite/PS/VL	7	Ilmenite 1g/L PS 0.5 mmol/L	20	Xia et al., 2018
E. coli	10^7	Single-atom Ru/PMS		Single-atom Ru 40 mg/L PMS 5 mg/L	1.5	Zhou et al., 2022
ARB E. coli	10^7	PS(PMS)/O_3	2	PS(PMS) 1 mg/L O_3 3 mg/L	10	Xiao et al., 2020

of PS. This is mainly due to the increase of sulfate radical. However, high concentrations of PS may also negatively affect the inactivation efficiency. This is mainly because excessive PS will quench $SO_4^{\bullet-}$ (Eqs. (4) and (5)), resulting in the formation of a critical PS concentration (Moreno-Andrés et al., 2019). For example, Venieri et al. (2020) showed that for the Fe^{2+}/PS system, the inactivation efficiency first increased with the increase of PS concentration, while the inactivation efficiency decreased instead when the PS concentration increased from 0.8 mmol/L to 1.3 mmol/L. Later, Wang et al. (2020a) introduced magnetic hydrochar (MHC) into the VL/PS system, and the results showed that the introduction of MHC enhances the inactivation rate

Table 3 Summary of inactivation of other bacteria by SR-AOPs

Microorganisms	Initial conc. (CFU/mL)	System	Max. Log removal value	Dosage	Exposure time (min)	Ref
E. faecalis	10^6	Fe^{3+}/PS	6	PS 200 mg/L Fe^{3+} 30 mg/L	15	Venieri et al., 2020
E. faecalis	10^6	50 °C/PS	2.5	PS 100 mg/L	180	Venieri et al., 2020
E. faecalis	10^6	UVA/PS	6	PS 300 mg/L	180	Venieri et al., 2020
E. faecalis	10^6	US/PS	6	PS 200 mg/L	120	Venieri et al., 2020
E. faecalis	10^7	ZVI/PS	6	PS 1 mmol/L ZVI 0.2 g/L	12	Liu et al., 2020
E. faecalis	10^6	PS/solar	6	PS 0.7 mmol/L	20	Ferreira et al., 2020
E. faecalis	10^6	solar/PS/ Fe(III)EDDS	5.6	PS 0.5 mmol/L Fe(III)EDDS 0.1 mmol/L	210	Bianco et al., 2017
B. subtilis	10^7	tris(2,2’-bipyridyl) ruthenium(II)/PS/hv	7	PS 2 mmol/L tris(2,2’-bipyridyl) ruthenium(II) 1 µmol/L	90	Subramanian et al., 2013
B. subtilis	10^6 to 10^8	PS/UV	4.1	PS 30 mmol/L	60	Sabeti et al., 2017
B. mycoides	10^3 to 10^4	UVA/PMS	2.82	0.1 mmol/L PMS	120	Rodríguez-Chueca et al., 2017a
B. mycoides	10^3 to 10^4	UVA/PMS/Fe^{2+}	2.51	0.1 mmol/L PMS 0.1 mmol/L Fe^{2+}	90	Rodríguez-Chueca et al., 2017a
B. mycoides	10^3 to 10^4	UVA/PMS/Co^{2+}	1.71	0.1 mmol/L PMS 0.1 mmol/L Co^{2+}	90	Rodríguez-Chueca et al., 2017a
B. mycoides	10^3 to 10^4	UVA/PMS/Co^{2+}	3.4	0.1 mmol/L PMS 0.1 mmol/L Co^{2+}	120	Rodríguez-Chueca et al., 2017b
B. mycoides	10^3 to 10^4	UVA/PMS/Fe^{2+}	3.2	0.1 mmol/L PMS 0.1 mmol/L Fe^{2+}	30	Rodríguez-Chueca et al., 2017b
S. aureus	10^8	VL/PS/MHC	8	MHC 200 mg/L PS 2 mmol/L	120	Wang et al., 2020a
S. aureus	10^7	CINMs/PMS	7	PMS 0.2 mmol/L	3	Shan et al., 2020
S. aureus	10^7	VL/PS	7	PS 2 mmol/L	200	Wang et al., 2019
S. aureus	10^7	tris(2,2’-bipyridyl) ruthenium(II)/PS/hv	7	PS 2 mmol/L tris(2,2’-bipyridyl) ruthenium(II) 1 µmol/L	60	Subramanian et al., 2013
S. aureus	10^3 to 10^4	UVA/PMS	4.02	0.1 mmol/L PMS	120	Rodríguez-Chueca et al., 2017a
S. aureus	10^3 to 10^4	UVA/PMS/Co^{2+}	3.14	0.1 mmol/L PMS 0.1 mmol/L Co^{2+}	120	Rodríguez-Chueca et al., 2017a
S. aureus	10^3 to 10^4	UVA/PMS/Fe^{2+}	2.84	0.1 mmol/L PMS 0.1 mmol/L Fe^{2+}	120	Rodríguez-Chueca et al., 2017a
S. aureus	10^3 to 10^4	UVA/PMS/Co^{2+}	6.1	0.1 mmol/L PMS 0.1 mmol/L Co^{2+}	120	Rodríguez-Chueca et al., 2017b
S. aureus	10^3 to 10^4	UVA/PMS/Fe^{2+}	3.2	0.1 mmol/L PMS 0.1 mmol/L Fe^{2+}	120	Rodríguez-Chueca et al., 2017b
S. aureus	10^7	NP/PS	7	PS 1 mmol/L NP 1.25 g/L	20	Xia et al., 2017
P. aeruginosa	10^8	VL/PS/MHC	8	MHC 200 mg/L PS 2 mmol/L	60	Wang et al., 2020a
P. aeruginosa	10^7	Cu(II)/PMS	3.4	Cu(II) 5 µmol/L PMS 0.2 mmol/L	20	Lee et al., 2020
P. aeruginosa	10^7	Cu(II)/PMS/Cl^-	3.1	Cu(II) 5 µmol/L PMS 0.2 mmol/L NaCl 10 mmol/L	10	Lee et al., 2020
P. aeruginosa	10^7	VL/PS	7	PS 2 mmol/L	140	Wang et al., 2019
P. aeruginosa	10^7	tris(2,2’-bipyridyl) ruthenium(II)/PS/hv	7	PS 2 mmol/L tris(2,2’-bipyridyl) ruthenium(II) 1 µmol/L	120	Subramanian et al., 2013
ARB pseudomonas sp.	10^8	UVC/PMS	5.3	PMS 1 mg/L	10	Hu et al., 2019b
Enterococcus sp.	10^6	$CoFe_2O_4$/PMS/UVA	6	$CoFe_2O_4$ 0.05 g/L PMS 0.2 mmol/L	45	Rodríguez-Chueca et al., 2020
Enterococcus sp.	10^6	PMS/UVA	6	PMS 1 mmol/L	90	Rodríguez-Chueca et al., 2019b

Table 4 Summary of fungus inactivation by SR-AOPs

Microorganisms	Initial conc. (CFU/mL)	System	Max. Log removal value	Dosage	Exposure time (min)	Ref
C. albicans	10^3 to 10^4	UVA/PMS	4.67	10 mmol/L PMS	15	Rodríguez-Chueca et al., 2017a
C. albicans	10^3 to 10^4	UVA/PMS/Fe^{2+}	1.41	10 mmol/L PMS 5 mmol/L Fe^{2+}	15	Rodríguez-Chueca et al., 2017a
C. albicans	10^3 to 10^4	UVA/PMS/Co^{2+}	3.64	10 mmol/L PMS 5 mmol/L Co^{2+}	15	Rodríguez-Chueca et al., 2017a
C. albicans	10^3 to 10^4	UVA/PMS/Co^{2+}	5.3	5 mmol/L PMS 2.5 mmol/L Co^{2+}	30	Rodríguez-Chueca et al., 2017b
C. albicans	10^3 to 10^4	UVA/PMS/Fe^{2+}	5	5 mmol/L PMS 2.5 mmol/L Fe^{2+}	60	Rodríguez-Chueca et al., 2017b
Acremonium sp.	(2–7)×10^5	PMS/UV	5	PMS 0.1 mmol/L	6	Wen et al., 2017
Acremonium sp.	(2–7)×10^5	PS/UV	3.7	PS 0.1 mmol/L	6	Wen et al., 2017
Cladosporium sp.	(2–7)×10^5	PMS/UV	4.9	PMS 0.1 mmol/L	15	Wen et al., 2017
Cladosporium sp.	(2–7)×10^5	PS/UV	3.9	PS 0.1 mmol/L	15	Wen et al., 2017
Penicillium sp.	(2–7)×10^5	PMS/UV	6.2	PMS 0.1 mmol/L	9	Wen et al., 2017
Penicillium sp.	(2–7)×10^5	PS/UV	5.9	PS 0.1 mmol/L	9	Wen et al., 2017
Trichoderma sp.	(2–7)×10^5	PMS/UV	5.2	PMS 0.1 mmol/L	6	Wen et al., 2017
Trichoderma sp.	(2–7)×10^5	PS/UV	5	PS 0.1 mmol/L	6	Wen et al., 2017

constant (k). *E. coli* in 8 log quantities were totally inactivated within 40 minutes. The k value increased from 0.19 min^{-1} in PS/MHC system to 0.99 min^{-1} in PS/MHC/VL system, and the inactivation efficiency increased by 5.21 times. The quenching experiments and EPR results showed that sulfate radical was the main free radical in PS/MHC and PS/MHC/VL systems. Moreover, the introduction of MHC led to a large increase in the concentration of sulfate radical and ultimately enhanced the inactivation efficiency.

$$S_2O_8^{2-} + SO_4^{\bullet-} \rightarrow S_2O_8^{\bullet-} + SO_4^{2-} \quad (4)$$

$$HSO_5^{-} + SO_4^{\bullet-} \rightarrow SO_5^{\bullet-} + HSO_4^{-} \quad (5)$$

Xiao et al. (2020) explored the inactivation kinetics of *E. faecalis* and *E. coli* by using zero-valent iron to activate PS. The pseudo-first-order inactivation rates for *E. faecalis* and *E. coli* to be 0.0924 min^{-1} and 0.0304 min^{-1}, respectively. In addition, they measured a second-order rate constant of (1.29–1.49)×10^9 $M^{-1}\cdot s^{-1}$ for *E. coli* and (6.61–6.81) ×10^9 $M^{-1}\cdot s^{-1}$ for *E. faecalis*. The results showed that the inactivation effect of $SO_4^{\bullet-}$ on Gram-positive bacterium was better than that of Gram-negative bacterium. Rodríguez-Chueca et al. (2019b) assessed the bacterial inactivation effect of homogeneous and heterogeneous Fe systems upon activation of PMS and PS under UV-A radiation. The experimental results showed that PMS system had better inactivation effect on bacteria than the PS system. Moreover, different Fe species had different inactivation effects on *E. coli* and *Enterococcus* sp. Among them, Fe(III)-citrate has a positive impact on the inactivation kinetics of *Enterococcus* sp. due to the production of additional oxidizing species such as superoxide radicals and hydrogen peroxide. In the heterogeneous system, compared with Fe_3O_4, nano-zero valent iron has inactivation effect on both bacteria, which is a very promising treatment method. In addition, some researchers have also explored the inactivation effects of magnetic pyrrhotite/PS (NP/PS) (Xia et al., 2017), S-mZVI/PS (Zhang et al., 2020) and $CoFe_2O_4$/PMS/UVA (Rodríguez-Chueca et al., 2020) systems on *E. coli*. The results show that these complex systems have enhancement of microorganism inactivation.

4 DBPs caused by SR-AOPs in water disinfection

As an economical and effective technique, SR-AOPs have received increasing attention in microorganisms inactivation. However, $SO_4^{\bullet-}$ will react with halide ions and convert them to reactive halogen species (RHS), which can be further oxidized to chlorates and bromates by the $SO_4^{\bullet-}$. RHS can also react with natural organic matter (NOM) and halogenated organic pollutants to form halogenated DBPs (Xie et al., 2016; Zhang et al., 2019). The conversion mechanism of halide ions when it co-exists with $SO_4^{\bullet-}$ is shown in Eqs. (6)–(11) (Wang et al., 2014; Hou et al., 2018; Chen et al., 2021). The maximum allowable concentration of BrO_3^- produced by the reaction of $SO_4^{\bullet-}$ with Br^- in drinking water in China, the USA, and Europe is 10 μg/L (Delker et al., 2006; Guan et al., 2020). For ClO_3^-, the health reference level recommended by the US EPA is 210 μg/L (Hou et al., 2018). Consequently, when use SR-AOPs for microbial inactivation, it is necessary to pay attention to the generated DBPs.

$$X^- + SO_4^{\bullet-} \rightarrow SO_4^{2-} + X^{\bullet} \quad (6)$$

$$X^{\bullet} + X^{-} \rightarrow X_2^{\bullet -} \quad (7)$$

$$X_2^{\bullet -} + X_2^{\bullet -} \rightarrow X_2 + 2X^{-} \quad (8)$$

$$X_2^{\bullet -} + X^{\bullet} \rightarrow X_2 + X^{-} \quad (9)$$

$$X_2 + H_2O \rightarrow H^{+} + HOX \quad (10)$$

$$X^{\bullet} + HOX \rightarrow XO^{\bullet} \quad (11)$$

4.1 $SO_4^{\bullet -}$ and bromide

In the presence of $SO_4^{\bullet -}$, the conversion of Br^- to BrO_3^- is shown in Fig. 2 (Guan et al., 2020). Fang and Shang (2012) proposed that hypobromous acid/hypobromite ($HOBr/OBr^-$) are the key intermediates in the transformation processes from Br^- to BrO_3^-. The same phenomenon has also been found by other researchers (Li et al., 2015; Huang et al., 2017; Wen et al., 2018).

The formation of BrO_3^- is highly dependent on the reaction conditions. Wang et al. (2020b) and Huang et al. (2017) found that the more BrO_3^- is formed at high temperature. This may be because the high temperature facilitates the formation of $SO_4^{\bullet -}$, and therefore more BrO_3^- is formed.

NOM is another important factor that affects the formation of BrO_3^-. Many studies have proved that NOM has an inhibitory effect on the formation of BrO_3^- in SR-AOPs (Liu et al., 2018). For example, Fang and Shang (2012) found that in actual water bodies with NOM, the amount of BrO_3^- produced is lower than that in ultrapure water. But there is still controversy regarding the suppression mechanism in the presence of NOM. Fang and Shang (2012) believe that there are two main reasons why NOM inhibits the formation of bromate: 1) NOM reacted with the generated reactive bromine species; and 2) NOM reacted with the generated $SO_4^{\bullet -}$ (Fang and Shang, 2012; Yang et al., 2019). In contrast, Lutze et al. (2014) have different ideas. In their study, they observed that no organic brominated by-products were formed. Therefore, they proposed that the inhibition of BrO_3^- formation is ascribed to the reduction of $HOBr/OBr^-$ by the $O_2^{\bullet -}$ formed by the reaction of $SO_4^{\bullet -}$ with NOM. Liu et al. (2018) believed that the main reason why NOM inhibited the formation of BrO_3^- was the reaction between NOM and $Br^{\bullet}$, which converted $Br^{\bullet}$ into Br^-. At the same time, they also believed that $O_2^{\bullet -}$ played an important role in inhibiting the generation of BrO_3^-. Interestingly, Lu et al. (2015) found organic bromination by-products, such as the formation of bromoacetic acid and bromoform, occurred in the study of bromide transformation during thermally activated oxidation process of PS in the presence of HA. Moreover, they found that when the $SO_4^{\bullet -}$ at a low concentration, some of the bromine was present in organic forms such as brominated disinfection by-products (Br-DBPs). When the PS concentration exceeded 5 mmol/L, the organic brominated by-products formed would eventually be converted into bromate. Similar phenomena also appeared in the works of Wang et al. (2020b) and Liu et al. (2015). In addition, pH will also affect the formation of BrO_3^-. For example, Li et al. (2015) explored the generation of BrO_3^- in the Co^{2+}/PMS system at different pH values. They found that when the pH increased from 2.7 to 6.3, more bromate was formed. On the contrary, when the pH increased from 6.3 to 9.5, the BrO_3^- formed decreased. Besides NOM and pH, there are many other factors affecting the formation of BrO_3^- and Br-DBPs, which need to be further explored.

4.2 $SO_4^{\bullet -}$ and chlorine

Chloride is ubiquitous in the aqueous environment, thus $SO_4^{\bullet -}$ will inevitably react with Cl^- in the process of disinfection. During the reaction of $SO_4^{\bullet -}$ and Cl^-, chlorine atoms ($Cl^{\bullet}$) are produced as intermediate products. Lutze et al. (2015) confirmed that regardless of the presence or absence of external conditions such as NOM, model organic matter or bicarbonate, pH had a great influence on $Cl^{\bullet}$ (Lutze et al., 2015; Ike et al., 2019). When the pH < 5, the $Cl^{\bullet}$ was converted to ClO_3^-. But when the pH > 5, the $Cl^{\bullet}$ mainly reacted with water to generate •OH (Eqs. (12)–(14)). It could be seen that under typical water treatment conditions of pH > 6, the formation of ClO_3^- could be ignored. Notably, they investigated that bicarbonate could scavenge $Cl^{\bullet}$ and interrupted the conversion of $SO_4^{\bullet -}$ to •OH.

$$Cl^{\bullet} + H_2O \rightarrow HOCl^{\bullet -} + H^{+} \quad (12)$$

$$HOCl^{\bullet -} \rightarrow {}^{\bullet}OH + Cl^{-} \quad (13)$$

$$Cl^{\bullet} + OH^{-} \rightarrow {}^{\bullet}OH + Cl^{-} \quad (14)$$

Thus far, the way in which Cl^- is converted to ClO_3^- during SR-AOPs is unclear. But it may be similar to the way Br^- forms BrO_3^-. Hou et al. (2018) found that in both cobalt (II)/ peroxymonosulfate (Co^{2+}/PMS) and UV/ persulfate (UV/PS) systems, the generation of ClO_3^- was associated with the formation of hypochlorous acid/hypochlorite ($HOCl/OCl^-$). In the UV/PS system, they found that the generation of $HOCl/OCl^-$ and ClO_3^- was mainly

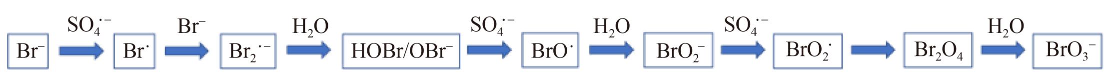

Fig. 2 Pathway of sulfate radical oxidation of Br^- to BrO_3^- (Guan et al., 2020) (Copyright 2020 Elsevier, Reprinted with permission from Elsevier).

attributed to $SO_4^{\bullet-}$. At the same time, they discovered that with the increase of Cl^-, more HOCl/OCl was produced, resulting in an increase in ClO_3^- production. However, the situation was slightly different in another system. In the Co/PMS system, Co^{3+} played an important role in the conversion of Cl^- into HOCl/OCl^-, and the formation of ClO_3^- was mainly ascribed to $SO_4^{\bullet-}$. At the same time, because of the high concentration of Cl^- accelerating the conversion of Co^{3+} to Co^{2+} (Eq. (15)), the generated Co^{2+} reacted with the $SO_4^{\bullet-}$ (Eq. (16)), resulting in the reduction of the $SO_4^{\bullet-}$, leading to the production of ClO_3^- increases first and then decreases.

$$Co^{3+} + Cl^- + H_2O \rightarrow Co^{2+} + HOCl/OCl^- \tag{15}$$

$$Co^{2+} + SO_4^{\bullet-} \rightarrow Co^{3+} + SO_4^{2-} \tag{16}$$

Hua et al. (2019) systematically studied the DBPs formed by NOM and five model compounds after UV/H_2O_2, UV/PS treatment and 24 hours' chlorination treatment. They found that the effect of UV/H_2O_2 treatment on the formation of DBPs was similar to that of UV/PS treatment, and the formation of DBPs after UV/H_2O_2 treatment was higher than that of UV/PS treatment. The change of DBPs after UV/PS treatment mainly depended on the structure of the precursor and the water matrix. Different precursors and water matrix structures could produce different DBPs and had different effects on DBPs. For example, after UV/PS treatment, the trichloromethane (TCM) and chloral hydrate (CH) formed by benzoic acid (BA) increased significantly, while the TCM and CH formed by resorcinol decreased significantly. In addition, they also found that the presence of inorganic ions will affect the generation of DBPs. For instance, the presence of chloride and bicarbonate increases the generation of Cl-DBPs. And the presence of bromide reduces the formation of Cl-DBPs but increases the production of Br-DBPs. Chen et al. (2021) explored the generation of CX_3R-type DBPs in the process of cobalt-catalyzed peroxymonosulfate (Co^{2+}/PMS) oxidation. They found that Co^{3+} played a major role in the formation of CX_3R-type DBPs and the conversion of chlorine to chlorate was mainly due to $SO_4^{\bullet-}$. It was worth noting that it could simultaneously produce and degrade CX_3R-type DBPs. In the degradation process, both $SO_4^{\bullet-}$ and Co^{3+} could convert CX_3R-type DBPs into chlorides, in which $SO_4^{\bullet-}$ played a major role.

4.3 $SO_4^{\bullet-}$ and iodide

The standard reduction potential of iodide (I^-) is 1.33 V, which is more easily oxidized by $SO_4^{\bullet-}$ than Cl^- and Br^- (Wang et al., 2017b). The reactive iodine species (RIS) after the oxidation of I^- can also react with NOM to generate iodinated DBPs (I-DBPs) such as iodoacetic acid (IAAs) and iodoform, which can cause odor and taste problems. Therefore, the formation of I-DBPs in the water disinfection process has been widely concerned. Wang et al. (2017b) used phenol to simulate NOM and investigated the conversion of I^- in the process of thermally activating PS. They discovered that I^- was converted into free iodine that attacks phenol, resulting in the formation of I-DBPs. Surprisingly, they observed that diiodoacetic acid (DIAA) was generated almost at the same time as iodophenol, and the generated DIAA was observably higher than triiodoacetic acid (TIAA), which was different from the traditional halogenation process. It indicated that there might be different ways of forming DIAA in this process. Contemporary, they also discovered that I-DBPs could react with excess $SO_4^{\bullet-}$ and converted to iodate (IO_3^-).

Hu et al. (2017) confirmed that pipe corrosion products (PCPs) can catalyze the degradation of iopamidol (IPM) by PMS. They found that most of I^- released from IPM was oxidized to IO_3^-, and a small part of the initial total organic iodine was converted to iodoform (CHI_3). And they also discovered that the water matrix would hinder the degradation of IPM. Similar conclusions were also proved in the degradation of IPM by the UV/PS system explored by Zhao et al. (2019b). The difference was that they noticed that $SO_4^{\bullet-}$ tended to oxidize the amino groups in IPM to nitro groups. At the same time, compared with the UV/H_2O_2 and UV/NaClO systems, the UV/NaClO system had the least potential for the generation of I-DBPs.

4.4 $SO_4^{\bullet-}$ and organohalogens

The composition of the water matrix is very complex, in addition to bromine, chlorine and iodine, there are many halogenated organic pollutants. They can also react with $SO_4^{\bullet-}$ to form DBPs. The DBPs formed by the reaction of sulfate radicals with halogenated organic pollutants can not be ignored. For example, When using Co(II) to activate PMS to degrade tetrabromobisphenol A (TBBPA), Ji et al. (2016) found that although $SO_4^{\bullet-}$ can effectively degrade TBBPA, reactive intermediates such as reactive bromine species (RBS) and 2,4,6-tribromophenol (TBP) were formed. The formed intermediates could be further oxidized by RBS to Br-DBP such as bromoacetic acid and bromoform. Surprisingly, DBPs were mainly generated after TBBPA was degraded. The production of bromoform and monobromoacetic acid reached the maximum after 6 h and 10 h, which were 177.8 μg/L and 38.4 μg/L, respectively. Afterwards, with the prolongation of the reaction time, the DBPs were degraded by $SO_4^{\bullet-}$ again.

When Xu et al. (2013) degraded 2,4,6-trichlorophenol (TCP) with Co^{2+}/PMS system, they found that the TCP degradation process would be accompanied by the generation of aromatic compounds such as 2,4,5-trichlorophenol and ring-opening products such as 2,4-

dichloro-5-oxygen-2-hexenoic acid. Anipsitakis et al. (2006) also found the formation of carbon tetrachloride in the same system. Zhao et al. (2019a) studied the degradation of iohexol in the Co^{2+}/PMS system under neutral conditions. The results showed that when 50 μmol/L iohexol was degraded by 1 mmol/L PMS and 1 μmol/L Co^{2+}, the CHI_3 and triiodoacetic acid produced within 12 h were 38.12 and 577.99 μg/L, respectively. Furthermore, the generation of I-DBP was significantly enhanced when HA was added. Hu et al. (2019a) also discovered the formation of CHI_3 when exploring the degradation of iohexol by the UV/PS system. The above works implies that attention should be paid to the generation of DBPs when using sulfate radicals to disinfect wastewater containing halogenated organic pollutants.

5 Future and challenge in $SO_4^{\bullet-}$ water disinfection techniques

In summary, the SR-AOPs technology has a very good inactivation efficiency for microorganisms. Compared with traditional water disinfection technology, it has broader application prospects. However, there are still many problems to be solved if the technology is applied in the actual disinfection process.

1) In the process of applying the SR-AOPs technology, its inactivation mechanism for microorganisms needs to be further explored. In various systems, it is necessary to explore the effect of experimental conditions such as the amount of disinfectant, temperature and pH on the inactivation efficiency. On this basis, the effect of actual water disinfection is explored. After that, pilot tests will be carried out to provide basis for large-scale application of this technology in practical water disinfection.

2) There are still many engineering challenges that must be solved before the full application of $SO_4^{\bullet-}$ water disinfection technology. For example, many metal catalysts and nano-material catalysts designed recent years have certain defects during the application process. Metal catalysts suffer from leakage of metal ions, and nanomaterial catalysts have the problem of high cost, which hinder their large-scale applications. Thus, in the actual application process, it is necessary to explore an efficient and economical activation method to increase the production of $SO_4^{\bullet-}$, so as to better inactivate microorganisms.

3) Before applying SR-AOPs for water disinfection treatment, the potential impact of this technology on the environment must be considered. If this method is used to disinfect water containing halogen ions such as Cl^- and Br^-, ClO_3^- and BrO_3^- will be generated. Meanwhile, when the water contains NOM, halogenated DBPs (such as Br-DBPs, Cl-DBPs and I-DBPs) will also be produced. Although compared with traditional disinfection technology, the formation of DBPs is much less, but a certain amount of DBPs will still be produced. Therefore, it is necessary to further explore the formation of BrO_3^-, ClO_3^-, IO_3^- and halogenated DBPs in the actual water body and the influence of other environmental factors such as inorganic ions and pH on the formation of these DBPs.

In order to reduce the DBPs produced by SR-AOPs in the water disinfection process, it can be achieved by adjusting the pH of the water body and adding bicarbonate/carbonate. Studies have shown that when pH > 5, $Cl^\bullet$ are more likely to be converted into •OH, thereby reducing the production of ClO_3^- (Lutze et al., 2015). At the same time, there are reports that the higher the pH, the slower the conversion of Br^- to $HOBr/BrO^-$. Therefore, increasing pH can reduce the formation rate of XO_3^- (Fang and Shang, 2012). Since bicarbonate/carbonate can quench $Cl^\bullet$ and their reaction rate with $SO_4^{\bullet-}$ is much slower than that of $Cl^\bullet$, bicarbonate/carbonate can be added into the system to reduce the formation of ClO_3^- (Mertens and von Sonntag, 1995). In addition, a novel catalyst can be developed to selectively remove XO_3^- and halogenated DBPs. It is also possible to introduce organic groups that can react with $X^\bullet$ in the catalyst, thereby effectively inhibiting the formation of XO_3^-.

Besides, in the process of applying the SR-AOPs technology, the generated SO_4^{2-} is another potential hazard. SO_4^{2-} is harmless at low concentrations, but when the concentration exceeds the limit value, they are corrosive. Moreover, exposure to high concentrations of SO_4^{2-} in swimming pool water can cause various intestinal diseases when it enters the intestine. Therefore, the concentration of SO_4^{2-} can be reduced by ion exchange or the addition of lime (Bougie and Dubé, 2007). In addition, crystallization/precipitation techniques can also be used when the SO_4^{2-} concentration are excessive (Tait et al., 2009).

Acknowledgements The study was financially supported by the Project of the National Key Research and Development Program of China (No. 2021YFC1910404), the National Natural Science Foundation of China (Nos. 52100008, 52100184, and 52100142), the Funds of Hunan Science and Technology Innovation Project (China) (Nos. 2021GK4055 and 2022SK2119), Natural Science Foundation of Hunan Province, China (No. 2021JJ40091), the Science and Technology Innovation Program of Hunan Province (China) (No. 2021RC2056), and the Project funded by China Postdoctoral Science Foundation (No. 2021M701149).

References

Anipsitakis G P, Dionysiou D D, Gonzalez M A (2006). Cobalt-mediated activation of peroxymonosulfate and sulfate radical attack on phenolic compounds: implications of chloride ions. Environmental Science & Technology, 40(3): 1000–1007

Anipsitakis G P, Tufano T P, Dionysiou D D (2008). Chemical and microbial decontamination of pool water using activated potassium peroxymonosulfate. Water Research, 42(12): 2899–2910

Ao X W, Eloranta J, Huang C H, Santoro D, Sun W J, Lu Z D, Li C (2021). Peracetic acid-based advanced oxidation processes for decontamination and disinfection of water: a review. Water Research, 188: 116479

Bai L, Jiang Y, Xia D, Wei Z, Spinney R, Dionysiou D D, Minakata D, Xiao R, Xie H B, Chai L (2022). Mechanistic understanding of superoxide radical-mediated degradation of perfluorocarboxylic acids. Environmental Science & Technology, 56(1): 624–633

Bianco A, Polo López M I, Fernández Ibáñez P, Brigante M, Mailhot G (2017). Disinfection of water inoculated with Enterococcus faecalis using solar/Fe(III)EDDS-H_2O_2 or $S_2O_8^{2-}$ process. Water Research, 118: 249–260

Bougie S, Dubé J (2007). Oxydation des isomères de dichlorobenzène à l'aide du persulfate de sodium soumis à une activation thermique. Journal of Environmental Engineering & Science, 6(4): 397–407(311)

Chen T T, Yu Z Y, Xu T, Xiao R, Chu W H, Yin D Q (2021). Formation and degradation mechanisms of CX_3R-type oxidation by-products during cobalt catalyzed peroxymonosulfate oxidation: The roles of Co^{3+} and SO_4 center dot. Journal of Hazardous Materials, 405: 124243

Cho M, Chung H, Choi W, Yoon J (2004). Linear correlation between inactivation of *E. coli* and OH radical concentration in TiO_2 photocatalytic disinfection. Water Research, 38(4): 1069–1077

Davies M J, Gilbert B C, Norman R (1984). Electron spin resonance. Part 67: Oxidation of aliphatic sulphides and sulphoxides by the sulphate radical anion ($SO_4^{-\cdot}$) and of aliphatic radicals by the peroxydisulphate anion ($S_2O_8^{2-}$). Journal of the Chemical Society, Perkin Transactions 2: Physical Organic Chemistry, (3): 503–509

Delker D, Hatch G, Allen J, Crissman B, George M, Geter D, Kilburn S, Moore T, Nelson G, Roop B, Slade R, Swank A, Ward W, DeAngelo A (2006). Molecular biomarkers of oxidative stress associated with bromate carcinogenicity. Toxicology, 221(2–3): 158–165

Devasagayam T P A, Tilak J C, Boloor K K, Sane K S, Ghaskadbi S S, Lele R D (2004). Free radicals and antioxidants in human health: current status and future prospects. Journal of the Association of Physicians of India, 52: 794–804

Fancy D A, Kodadek T (1999). Chemistry for the analysis of protein-protein interactions: rapid and efficient cross-linking triggered by long wavelength light. Proceedings of the National Academy of Sciences of the United States of America, 96(11): 6020–6024

Fang J Y, Shang C (2012). Bromate formation from bromide oxidation by the UV/persulfate process. Environmental Science & Technology, 46(16): 8976–8983

Ferreira L C, Castro-Alferez M, Nahim-Granados S, Polo-Lopez M I, Lucas M S, Li Puma G, Fernandez-Ibanez P (2020). Inactivation of water pathogens with solar photo-activated persulfate oxidation. Chemical Engineering Journal, 381: 122275

Garkusheva N, Matafonova G, Tsenter I, Beck S, Batoev V, Linden K (2017). Simultaneous atrazine degradation and E-coli inactivation by simulated solar photo-Fenton-like process using persulfate. Journal of Environmental Science and Health Part A: Toxic/Hazardous Substances & Environmental Engineering, 52(9): 849–855

Gau B C, Chen H, Zhang Y, Gross M L (2010). Sulfate radical anion as a new reagent for fast photochemical oxidation of proteins. Analytical Chemistry, 82(18): 7821–7827

Ghanbari F, Moradi M (2017). Application of peroxymonosulfate and its activation methods for degradation of environmental organic pollutants. Chemical Engineering Journal, 310: 41–62

Guan C, Jiang J, Pang S, Zhou Y, Gao Y, Li J, Wang Z (2020). Formation and control of bromate in sulfate radical-based oxidation processes for the treatment of waters containing bromide: a critical review. Water Research, 176: 115725

Guerra-Rodríguez S, Rodríguez E, Singh D N, Rodríguez-Chueca J (2018). Assessment of sulfate radical-based advanced oxidation processes for water and wastewater treatment: a review. Water, 10(12): 1828

Hou S D, Ling L, Dionysiou D D, Wan Y R, Huang J J, Guo K H, Li X C, Fang J Y (2018). Chlorate formation mechanism in the presence of sulfate radical, chloride, bromide and natural organic matter. Environmental Science & Technology, 52(11): 6317–6325

Hu C Y, Hou Y Z, Lin Y L, Deng Y G, Hua S J, Du Y F, Chen C W, Wu C H (2019a). Kinetics and model development of iohexol degradation during UV/H_2O_2 and UV/$S_2O_8^{2-}$ oxidation. Chemosphere, 229: 602–610

Hu J, Dong H, Qu J, Qiang Z (2017). Enhanced degradation of iopamidol by peroxymonosulfate catalyzed by two pipe corrosion products (CuO and δ-MnO_2). Water Research, 112: 1–8

Hu L, Wang P, Shen T, Wang Q, Wang X, Xu P, Zheng Q, Zhang G (2020). The application of microwaves in sulfate radical-based advanced oxidation processes for environmental remediation: a review. Science of the Total Environment, 722: 137831

Hu P D, Long M C (2016). Cobalt-catalyzed sulfate radical-based advanced oxidation: A review on heterogeneous catalysts and applications. Applied Catalysis B: Environmental, 181: 103–117

Hu Y R, Zhang T Y, Jiang L, Yao S J, Ye H, Lin K F, Cui C Z (2019b). Removal of sulfonamide antibiotic resistant bacterial and intracellular antibiotic resistance genes by UVC-activated peroxymonosulfate. Chemical Engineering Journal, 368: 888–895

Hua Z, Kong X, Hou S, Zou S, Xu X, Huang H, Fang J (2019). DBP alteration from NOM and model compounds after UV/persulfate treatment with post chlorination. Water Research, 158: 237–245

Huang X, Zhou X, Zhou J, Huang Z, Liu S, Qian G, Gao N (2017). Bromate inhibition by reduced graphene oxide in thermal/PMS process. Water Research, 122: 701–707

Huie R E, Clifton C L (1993). Kinetics of the self-reaction of hydroxymethylperoxyl radicals. Chemical Physics Letters, 205(2–3): 163–167

Ike I A, Karanfil T, Cho J, Hur J (2019). Oxidation byproducts from the degradation of dissolved organic matter by advanced oxidation processes - A critical review. Water Research, 164: 114929

Ji Y, Kong D, Lu J, Jin H, Kang F, Yin X, Zhou Q (2016). Cobalt catalyzed peroxymonosulfate oxidation of tetrabromobisphenol A: kinetics, reaction pathways, and formation of brominated by-products. Journal of Hazardous Materials, 313: 229–237

Lee H J, Kim H E, Kim M S, De Lannoy C F, Lee C (2020). Inactivation of bacterial planktonic cells and biofilms by Cu(II)-activated peroxymonosulfate in the presence of chloride ion. Chemical Engineering Journal, 380: 122468

Lei X, Lei Y, Zhang X, Yang X (2021). Treating disinfection byproducts with UV or solar irradiation and in UV advanced oxidation processes: a review. Journal of Hazardous Materials, 408: 124435

Lei Y, Chen C S, Tu Y J, Huang Y H, Zhang H (2015). Heterogeneous degradation of organic pollutants by persulfate activated by CuO-Fe_3O_4: mechanism, stability, and effects of pH and bicarbonate ions. Environmental Science & Technology, 49(11): 6838–6845

Li Z, Chen Z, Xiang Y, Ling L, Fang J, Shang C, Dionysiou D D (2015). Bromate formation in bromide-containing water through the cobalt-mediated activation of peroxymonosulfate. Water Research, 83: 132–140

Lian L, Yao B, Hou S, Fang J, Yan S, Song W (2017). Kinetic study of hydroxyl and sulfate radical-mediated oxidation of pharmaceuticals in wastewater effluents. Environmental Science & Technology, 51(5): 2954–2962

Liang J H, Gao P, Li B H, Kang L F, Feng L, Han Q, Liu Y Z, Zhang L Q (2022). Characteristics of typical dissolved black carbons and their influence on the formation of disinfection by-products in chlor(am)ination. Frontiers of Environmental Science & Engineering, 16(12): 150

Liu K, Bai L, Shi Y, Wei Z S, Spinney R, Goktas R K, Dionysiou D D, Xiao R Y (2020). Simultaneous disinfection of *E. faecalis* and degradation of carbamazepine by sulfate radicals: an experimental and modelling study. Environmental Pollution, 263: 114558

Liu K, Lu J, Ji Y (2015). Formation of brominated disinfection by-products and bromate in cobalt catalyzed peroxymonosulfate oxidation of phenol. Water Research, 84: 1–7

Liu Y Z, Yang Y, Pang S Y, Zhang L Q, Ma J, Luo C W, Guan C T, Jiang J (2018). Mechanistic insight into suppression of bromate formation by dissolved organic matters in sulfate radical-based advanced oxidation processes. Chemical Engineering Journal, 333: 200–205

Lu J, Wu J, Ji Y, Kong D (2015). Transformation of bromide in thermo activated persulfate oxidation processes. Water Research, 78: 1–8

Lutze H V, Bakkour R, Kerlin N, von Sonntag C, Schmidt T C (2014). Formation of bromate in sulfate radical based oxidation: mechanistic aspects and suppression by dissolved organic matter. Water Research, 53: 370–377

Lutze H V, Kerlin N, Schmidt T C (2015). Sulfate radical-based water treatment in presence of chloride: formation of chlorate, inter-conversion of sulfate radicals into hydroxyl radicals and influence of bicarbonate. Water Research, 72: 349–360

Ma H K, Zhang L L, Huang X M, Ding W, Jin H, Li Z F, Cheng S K, Zheng L (2019). A novel three-dimensional galvanic cell enhanced Fe^{2+}/persulfate system: High efficiency, mechanism and damaging effect of antibiotic resistant E-coli and genes. Chemical Engineering Journal, 362: 667–678

Marjanovic M, Giannakis S, Grandjean D, de Alencastro L F, Pulgarin C (2018). Effect of μM Fe addition, mild heat and solar UV on sulfate radical-mediated inactivation of bacteria, viruses, and micropollutant degradation in water. Water Research, 140: 220–231

Mertens R, von Sonntag C (1995). Photolysis (λ = 354 nm) of tetrachloroethene in aqueous solutions. Journal of Photochemistry and Photobiology A: Chemistry, 85(1–2): 1–9

Michael-Kordatou I, Iacovou M, Frontistis Z, Hapeshi E, Dionysiou D D, Fatta-Kassinos D (2015). Erythromycin oxidation and ERY-resistant *Escherichia coli* inactivation in urban wastewater by sulfate radical-based oxidation process under UV-C irradiation. Water Research, 85: 346–358

Moreno-Andrés J, Farinango G, Romero-Martínez L, Acevedo-Merino A, Nebot E (2019). Application of persulfate salts for enhancing UV disinfection in marine waters. Water Research, 163: 114866

Neta P, Huie R E, Ross A B (1988). Rate constants for reactions of inorganic radicals in aqueous solution. Journal of Physical and Chemical Reference Data, 17(3): 1027–1284

Oh W D, Dong Z L, Lim T T (2016). Generation of sulfate radical through heterogeneous catalysis for organic contaminants removal: current development, challenges and prospects. Applied Catalysis B: Environmental, 194: 169–201

Pignatello J J, Oliveros E, Mackay A (2006). Advanced oxidation processes for organic contaminant destruction based on the Fenton reaction and related chemistry. Critical Reviews in Environmental Science and Technology, 36(1): 1–84

Qi W H, Zhu S M, Shitu A, Ye Z Y, Liu D Z (2020). Low concentration peroxymonosulfate and UVA-LED combination for *E. coli* inactivation and wastewater disinfection from recirculating aquaculture systems. Journal of Water Process Engineering, 36: 101362

Richardson S D, Kimura S Y (2019). Water analysis: emerging contaminants and current issues. Analytical Chemistry, 92(1): 473–505

Rodríguez-Chueca J, Barahona-Garcia E, Blanco-Gutierrez V, Isidoro-Garcia L, Dos Santos-Garcia A J (2020). Magnetic $CoFe_2O_4$ ferrite for peroxymonosulfate activation for disinfection of wastewater. Chemical Engineering Journal, 398: 125606

Rodríguez-Chueca J, Giannakis S, Marjanovic M, Kohantorabi M, Gholami M R, Grandjean D, De Alencastro L F, Pulgarin C (2019a). Solar-assisted bacterial disinfection and removal of contaminants of emerging concern by Fe^{2+}-activated HSO_5^- vs. $S_2O_8^{2-}$ in drinking water. Applied Catalysis B: Environmental, 248: 62–72

Rodríguez-Chueca J, Guerra-Rodriguez S, Raez J M, Lopez-Munoz M J, Rodriguez E (2019b). Assessment of different iron species as activators of $S_2O_8^{2-}$ and HSO_5^- for inactivation of wild bacteria strains. Applied Catalysis B: Environmental, 248: 54–61

Rodríguez-Chueca J, Moreira S I, Lucas M S, Fernandes J R, Tavares P B, Sampaio A, Peres J A (2017a). Disinfection of simulated and real winery wastewater using sulphate radicals: peroxymonosulphate/transition metal/UV-A LED oxidation. Journal of Cleaner Production, 149: 805–817

Rodríguez-Chueca J, Silva T, Fernandes J R, Lucas M S, Puma G L, Peres J A, Sampaio A (2017b). Inactivation of pathogenic microorganisms in freshwater using HSO_5^-/UV-A LED and HSO_5^-/M^{n+}/UV-A LED oxidation processes. Water Research, 123: 113–123

Roginskaya M, Mohseni R, Ampadu-Boateng D, Razskazovskiy Y (2016). DNA damage by the sulfate radical anion: hydrogen abstraction from the sugar moiety versus one-electron oxidation of guanine. Free Radical Research, 50(7): 756–766

Sabeti Z, Alimohammadi M, Yousefzadeh S, Aslani H, Ghani M, Nabizadeh R (2017). Application of response surface methodology for modeling and optimization of *Bacillus subtilis* spores inactivation by the UV/persulfate process. Water Science and Technology: Water Supply, 17(2): 342–351

Shan H R, Si Y, Yu J Y, Ding B (2020). Flexible, mesoporous, and monodispersed metallic cobalt-embedded inorganic nanofibrous membranes enable ultra-fast and high-efficiency killing of bacteria. Chemical Engineering Journal, 382: 122909

Sonntag C (2006). Free-Radical-Induced DNA Damage and Its Repair: A Chemical Perspective. Berlin: Springer Science & Business Media

Subramanian G, Parakh P, Prakash H (2013). Photodegradation of methyl orange and photoinactivation of bacteria by visible light activation of persulphate using a tris(2,2′-bipyridyl)ruthenium(II) complex. Photochemical & Photobiological Sciences, 12(3): 456–466

Sun P, Tyree C, Huang C H (2016). Inactivation of *Escherichia coli*, bacteriophage MS_2, and *Bacillus* spores under UV/H_2O_2 and UV/peroxydisulfate advanced disinfection conditions. Environmental Science & Technology, 50(8): 4448–4458

Tait S, Clarke W P, Keller J, Batstone D J (2009). Removal of sulfate from high-strength wastewater by crystallisation. Water Research, 43(3): 762–772

Tang J L, Wang J J, Tang L, Feng C Y, Zhu X, Yi Y Y, Feng H P, Yu J F, Ren X Y (2022). Preparation of floating porous g-C_3N_4 photocatalyst via a facile one-pot method for efficient photocatalytic elimination of tetracycline under visible light irradiation. Chemical Engineering Journal, 430: 132669

Venieri D, Karapa A, Panagiotopoulou M, Gounaki I (2020). Application of activated persulfate for the inactivation of fecal bacterial indicators in water. Journal of Environmental Management, 261: 110223

Wacławek S, Lutze H V, Grubel K, Padil V V T, Cernik M, Dionysiou D D (2017). Chemistry of persulfates in water and wastewater treatment: a review. Chemical Engineering Journal, 330: 44–62

Waldemer R H, Tratnyek P G, Johnson R L, Nurmi J T (2007). Oxidation of chlorinated ethenes by heat-activated persulfate: kinetics and products. Environmental Science & Technology, 41(3): 1010–1015

Wang H, Ma D F, Shi W Y, Yang Z Y, Cai Y, Gao B Y (2021). Formation of disinfection by-products during sodium hypochlorite cleaning of fouled membranes from membrane bioreactors. Frontiers of Environmental Science & Engineering, 15(5): 102

Wang J, Chen H, Tang L, Zeng G, Liu Y, Yan M, Deng Y, Feng H, Yu J, Wang L (2018). Antibiotic removal from water: A highly efficient silver phosphate-based Z-scheme photocatalytic system under natural solar light. Science of the Total Environment, 639: 1462–1470

Wang J J, Tang L, Zeng G M, Deng Y C, Liu Y N, Wang L G, Zhou Y Y, Guo Z, Wang J J, Zhang C (2017a). Atomic scale g-C_3N_4/Bi_2WO_6 2D/2D heterojunction with enhanced photocatalytic degradation of ibuprofen under visible light irradiation. Applied Catalysis B: Environmental, 209: 285–294

Wang J L, Wang S Z (2018). Activation of persulfate (PS) and peroxymonosulfate (PMS) and application for the degradation of emerging contaminants. Chemical Engineering Journal, 334: 1502–1517

Wang L, Kong D, Ji Y, Lu J, Yin X, Zhou Q (2017b). Transformation of iodide and formation of iodinated by-products in heat activated persulfate oxidation process. Chemosphere, 181: 400–408

Wang W, Wang H, Li G, An T, Zhao H, Wong P K (2019). Catalyst-free activation of persulfate by visible light for water disinfection: Efficiency and mechanisms. Water Research, 157: 106–118

Wang W, Wang H, Li G, Wong P K, An T (2020a). Visible light activation of persulfate by magnetic hydrochar for bacterial inactivation: efficiency, recyclability and mechanisms. Water Research, 176: 115746

Wang Y, Le Roux J, Zhang T, Croué J P (2014). Formation of brominated disinfection byproducts from natural organic matter isolates and model compounds in a sulfate radical-based oxidation process. Environmental Science & Technology, 48(24): 14534–14542

Wang Z Y, Shao Y S, Gao N Y, Xu B, An N, Lu X (2020b). Comprehensive study on the formation of brominated byproducts during heat-activated persulfate degradation. Chemical Engineering Journal, 381: 122660

Wen G, Qiang C, Feng Y B, Huang T L, Ma J (2018). Bromate formation during the oxidation of bromide-containing water by ozone/peroxymonosulfate process: Influencing factors and mechanisms. Chemical Engineering Journal, 352: 316–324

Wen G, Xu X Q, Zhu H, Huang T L, Ma J (2017). Inactivation of four genera of dominant fungal spores in groundwater using UV and UV/PMS: efficiency and mechanisms. Chemical Engineering Journal, 328: 619–628

Wu X, Xu G, Zhu J J (2019). Sonochemical synthesis of Fe_3O_4/carbon nanotubes using low frequency ultrasonic devices and their performance for heterogeneous sono-persulfate process on inactivation of *Microcystis aeruginosa*. Ultrasonics Sonochemistry, 58: 104634

Xia D, Li Y, Huang G, Yin R, An T, Li G, Zhao H, Lu A, Wong P K (2017). Activation of persulfates by natural magnetic pyrrhotite for water disinfection: efficiency, mechanisms, and stability. Water Research, 112: 236–247

Xia D H, He H J W, Liu H D, Wang Y C, Zhang Q, Li Y, Lu A H, He C, Wong P K (2018). Persulfate-mediated catalytic and photocatalytic bacterial inactivation by magnetic natural ilmenite. Applied Catalysis B: Environmental, 238: 70–81

Xia D H, Tang Z Y, Wang Y C, Yin R, He H J W, Xie X, Sun J L, He C, Wong P K, Zhang G (2020). Piezo-catalytic persulfate activation system for water advanced disinfection: process efficiency and inactivation mechanisms. Chemical Engineering Journal, 400: 125894

Xiao R, Bai L, Liu K, Shi Y, Minakata D, Huang C H, Spinney R, Seth R, Dionysiou D D, Wei Z, Sun P (2020). Elucidating sulfate radical-mediated disinfection profiles and mechanisms of *Escherichia coli* and *Enterococcus faecalis* in municipal wastewater. Water Research, 173: 115552

Xiao R Y, Liu K, Bai L, Minakata D, Seo Y, Göktaş R K, Dionysiou D D, Tang C J, Wei Z S, Spinney R (2019). Inactivation of pathogenic microorganisms by sulfate radical: present and future. Chemical Engineering Journal, 371: 222–232

Xiao R Y, Luo Z H, Wei Z S, Luo S, Spinney R, Yang W C, Dionysiou D D (2018). Activation of peroxymonosulfate/persulfate by nanomaterials for sulfate radical-based advanced oxidation technologies. Current Opinion in Chemical Engineering, 19: 51–58

Xie W, Dong W, Kong D, Ji Y, Lu J, Yin X (2016). Formation of halogenated disinfection by-products in cobalt-catalyzed peroxymonosulfate oxidation processes in the presence of halides. Chemosphere, 154: 613–619

Xu L, Yuan R X, Guo Y G, Xiao D X, Cao Y, Wang Z H, Liu J S (2013). Sulfate radical-induced degradation of 2,4,6-trichlorophenol: a de novo formation of chlorinated compounds. Chemical Engineering Journal, 217: 169–173

Yang J, Dong Z, Jiang C, Wang C, Liu H (2019). An overview of bromate formation in chemical oxidation processes: occurrence, mechanism, influencing factors, risk assessment, and control strategies. Chemosphere, 237: 124521

Yang S, Wang P, Yang X, Shan L, Zhang W, Shao X, Niu R (2010). Degradation efficiencies of azo dye Acid Orange 7 by the interaction of heat, UV and anions with common oxidants: persulfate, peroxymonosulfate and hydrogen peroxide. Journal of Hazardous Materials, 179(1–3): 552–558

Yu J F, Feng H P, Tang L, Pang Y, Zeng G M, Lu Y, Dong H R, Wang J J, Liu Y N, Feng C Y, Wang J J, Peng B, Ye S J (2020). Metal-free carbon materials for persulfate-based advanced oxidation process: microstructure, property and tailoring. Progress in Materials Science, 111: 100654

Zhang A, Wang F, Chu W, Yang X, Pan Y, Zhu H (2019). Integrated control of CX_3R-type DBP formation by coupling thermally activated persulfate pre-oxidation and chloramination. Water Research, 160: 304–312

Zhang C, Li Y, Wang C, Zheng X (2021). Different inactivation behaviors and mechanisms of representative pathogens (*Escherichia coli* bacteria, human adenoviruses and *Bacillus subtilis* spores) in g-C_3N_4-based metal-free visible-light-enabled photocatalytic disinfection. Science of the Total Environment, 755(Pt 1): 142588

Zhang L L, Jin H, Ma H K, Gregory K, Qi Z W, Wang C X, Wu W T, Cang D Q, Li Z F (2020). Oxidative damage of antibiotic resistant *E. coli* and gene in a novel sulfidated micron zero-valent activated persulfate system. Chemical Engineering Journal, 381: 122787

Zhang L S, Wong K H, Yip H Y, Hu C, Yu J C, Chan C Y, Wong P K (2010). Effective photocatalytic disinfection of *E. coli* K-12 using AgBr-Ag-Bi_2WO_6 nanojunction system irradiated by visible light: the role of diffusing hydroxyl radicals. Environmental Science & Technology, 44(4): 1392–1398

Zhang Y, Zhou L, Zhang Y, Tan C (2014). Inactivation of *Bacillus subtilis* spores using various combinations of ultraviolet treatment with addition of hydrogen peroxide. Photochemistry and Photobiology, 90(3): 609–614

Zhao H, Huang C H, Zhong C, Du P H, Sun P Z (2022). Enhanced formation of trihalomethane disinfection byproducts from halobenzoquinones under combined UV/chlorine conditions. Frontiers of Environmental Science & Engineering, 16(6): 76

Zhao H X, Ji Y F, Kong D Y, Lu J H, Yin X M, Zhou Q S (2019a). Degradation of iohexol by Co^{2+} activated peroxymonosulfate oxidation: kinetics, reaction pathways, and formation of iodinated byproducts. Chemical Engineering Journal, 373: 1348–1356

Zhao X, Jiang J, Pang S, Guan C, Li J, Wang Z, Ma J, Luo C (2019b). Degradation of iopamidol by three UV-based oxidation processes: kinetics, pathways, and formation of iodinated disinfection byproducts. Chemosphere, 221: 270–277

Zhou S, Bu L, Shi Z, Deng L, Zhu S, Gao N (2018). Electrochemical inactivation of *Microcystis aeruginosa* using BDD electrodes: kinetic modeling of microcystins release and degradation. Journal of Hazardous Materials, 346: 73–81

Zhou X, Yang Z Z, Chen Y, Feng H P, Yu J F, Tang J L, Ren X Y, Tang J, Wang J J, Tang L (2022). Single-atom Ru loaded on layered double hydroxide catalyzes peroxymonosulfate for effective *E. coli* inactivation via a non-radical pathway: efficiency and mechanism. Journal of Hazardous Materials, 440: 129720